A band model for the electronic and magnetic structure of $NaCrS_2$

1989 J. Phys.: Condens. Matter 1 5653

(http://iopscience.iop.org/0953-8984/1/33/008)

J. Phys.: Condens. Matter 1 (1989) 5653–5666. Printed in the UK

A band model for the electronic and magnetic structure of $NaCrS_2$

D Sébilleau†, G Y Guo and W M Temmerman
SERC Daresbury Laboratory, Warrington WA4 4AD, UK

Received 26 September 1988, in final form 2 February 1989

Abstract. We have performed local density calculations for $NaCrS_2$ with the LMTO–ASA method. We have studied the electronic structure and ground state properties of $NaCrS_2$ in the 3R and the hypothetical 1T structure. The magnetic properties have been studied within the framework of the local spin-density approximation. We obtain a semiconducting antiferromagnetic ground state with a moment of 3 μ_B per Cr atom. The electronic band structure is compared with photoemission and optical measurements.

1. Introduction

There has been considerable interest over the last decade in the study of transition-metal dichalcogenides and their intercalated complexes because they show a wide range of very different physical properties and have found numerous technical applications (see, e.g., Friend and Yoffe (1987), and Liang (1986) and references therein). These crystals are known to be highly anisotropic and most of them exhibit a strong two-dimensional character as a result of their layer-type structures with weak bonding between the layers. More precisely, they consist of a stacking of TX_2 (T: transition metal; X: chalcogen) sandwiches separated by a van der Waals gap where intercalant species (mostly electron donors) such as alkali atoms, organic molecules and 3d transition-metal atoms can be inserted. Hence $NaCrS_2$ can be viewed as a Na-intercalated transition-metal dichalcogenide, although the compound CrS_2 is not known to exist; however, the less ionic $CrSe_2$ has recently been synthesised (van Bruggen *et al* 1980) and was found to have exactly the same structure as $NaCrS_2$ when intercalated with Na. $NaCrS_2$ is a semiconductor with a direct optical band gap of 2.16 eV and is antiferromagnetic below 19 K (Bongers *et al* 1968). Its exact magnetic structure has been subject to controversy. The actual picture (Engelsman *et al* 1973) consists of ferromagnetic layers that are antiferromagnetically coupled with a type of helical arrangement of the spins within a layer. From the application of Hund's rules, it is expected that there will be a spin-only moment of $3\mu_B$. Magnetic measurements by Blazey and Rohrer (1969) and photoemission results by Hughes *et al* (1981) have confirmed this value.

Although many band-structure calculations of layered materials have been performed (see the references in the review articles of Friend and Yoffe 1987 and Liang 1986), most of the work has been focused on the understanding of the formation of periodic lattice-distortion–charge-density waves (PLD–CDW), and it is only recently that

† Present address: LURE, Bâtiment 209d, Université de Paris-Sud, 91405 Orsay Cédex, France.

0953-8984/89/335653 + 14 $02.50

self-consistent band-structure calculations of transition-metal dichalcogenides have been carried out (see for example Benesh *et al* 1985 and Guo and Liang 1987 and references therein). Many features in the optical, electrical and photoemission data collected from the intercalate complexes of the transition-metal dichalcogenides have been explained using the simple rigid-band model (Wilson and Yoffe 1969). In the case of $NaCrS_2$, Khumalo and Hughes (1980) have derived from their optical measurements an improved version of the rigid-band model, according to which the chromium 3d orbital form discrete localised states within a gap between the s, p valence band and the Cr4s conduction band, and these discrete Cr3d states are split due to the octahedral ligand field. Even if this qualitative model has proved useful, a reliable electronic-structure picture is essential to the understanding of the electronic and magnetic properties of chromium sodium disulphide. In particular, we would want to give a unified and quantitative description of the localised and band-like features of $NaCrS_2$.

The presence of localised and band-like states in $NaCrS_2$ might make the reader circumspect concerning the applicability of band theory to the study of this material. However, band calculations have been able to describe the transition from band-like to localised behaviour successfully, in the 5f actinides or 3d monoxides for example, as well as their groundstate properties (Andersen *et al* 1985). We also note that a simple Mott–Hubbard picture is not applicable for this material since the exchange coupling is highly anisotropic, favouring a parallel alignment of the spins in the layers and a much more complicated antiferromagnetic coupling between the layers. In this paper we report on spin-polarised band-structure calculations of this magnetic layered compound.

In the next section, we briefly describe the 3R crystal structure and the hypothetical 1T structure. This is then followed by a short account of our computational method. We present the results of our work in § 3 and discuss the band structures and densities of states of the non-magnetic, ferromagnetic and antiferromagnetic structures of both the 1T and 3R polytypes. The fourth section is devoted to the study of the energetics and the bonding of the various structures. Our results are compared with available experimental data in § 5.

2. Computational details

2.1. Crystal structure

The crystal structure of $NaCrS_2$ has been reported by Rüdorff and Stegemann (1943) and then refined by Bongers *et al* (1968) and Engelsman *et al* (1973). It can be viewed (figure 1) as a stacking of alternate hexagonal layers of Cr, S and Na, arranged along the c axis in the sequence Cr–S–Na–S–Cr. The Na ions are situated in octahedral holes between the CrS_2 sandwiches, and within a sandwich the Cr ions occupy octahedral sites. It belongs to the rhombohedral system with the space group $R\bar{3}m$–D_{3d}^5 and it is often referred to as a 3R structure because its unit cell contains three sandwich layers. With respect to the trigonal axes, the atoms are located at the following positions: Cr: $(0,0,0)$; Na: $(0,0,\frac{1}{2})$; S: $\pm(0,0,z)$. The basic parameters of the unit cell, at $T = 4.2$ K, are listed in table 1 (after Engelsman *et al* 1973). As already mentioned, the coupling between the layers is expected to be small compared with the interactions between the atoms within a layer. Therefore the band structure must be dominated by the arrangement of the atoms within the layers and it seems to be a reasonable approximation, in a first step, to slightly alter the position of the layers with respect to one

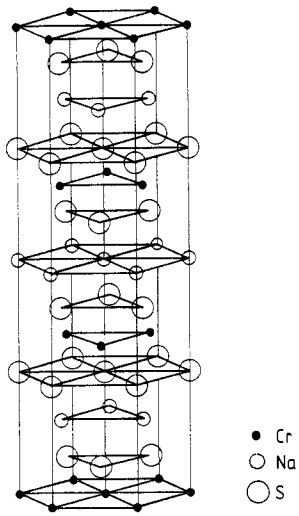

Figure 1. Structure of 3R $NaCrS_2$.

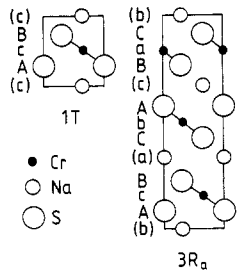

Figure 2. Unit cells of 1T and 3R polytypes of $NaCrS_2$ in (1120) planes (see text).

Table 1. Structural parameters of $NaCrS_2$.

a	c	c/a	V	z
3.5561 Å	19.365 Å	5.446	212.3 Å^3	0.2667

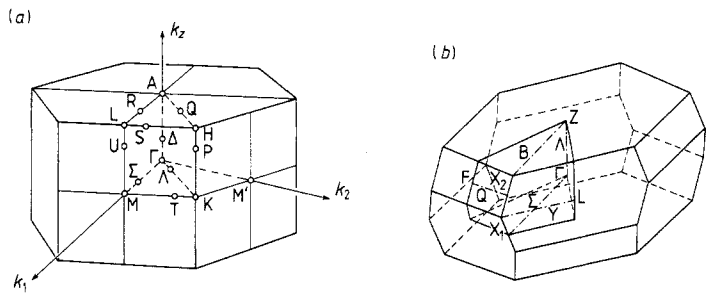

Figure 3. The Brillouin zones for (*a*) 1T and (*b*) 3R crystal structures.

another in order to reduce the 3R unit cell into a simpler 1T one which is three times smaller. Figure 2 shows a section of these two unit cells through the $(11\bar{2}0)$ planes. We note that in this figure the unit cell of the 3R structure is non-primitive. Indeed, its actual primitive cell is rhombohedral, with a c axis not perpendicular to the layer plane.

We have used both the hypothetical 1T and the real 3R structures in our calculations. The corresponding Brillouin zones are shown in figure 3, where the irreducible wedges have also been represented.

2.2. Band structure method

The ground-state electronic properties of $NaCrS_2$ have been obtained from an effective one-electron approach within the density-functional theory (Hohenberg and Kohn 1964). We have used the von Barth–Hedin local-density form for the exchange and correlation potential (Kohn and Sham 1965, von Barth and Hedin 1972). The Lagrange multipliers of the effective one-electron Kohn–Sham equation are identified as the energy bands. This is often a very useful approximation for the excitation spectrum of solids, as has been demonstrated by, for example, the angle-resolved photoemission measurement that succeeded in determining most of the occupied states for Cu (Thiry *et al* 1977). This approach is, however, less valid when the energy bands become narrow (Jordan and Durham 1989).

The band structure method we have used is the LMTO–ASA (Andersen 1984, Skriver 1984), linear muffin-tin orbital in the atomic sphere approximation pioneered by O K Anderson (1975). It is a fast and physically transparent band-structure method, used at the expense only of small loss in accuracy. This allows us to study the electronic structure of complicated systems such as the antiferromagnetic layer compound on which we report in this paper.

We have performed SCF–LMTO–ASA calculations for various Wigner–Seitz spheres in order to obtain the theoretrical lattice constant and, moreover, in the non-magnetic, the ferromagnetic and the antiferromagnetic structures. The frozen-core approximation has been used in all the calculations. The scalar-relativistic Hamiltonian has been solved without the spin–orbit coupling. As the sodium and sulphur d bands lie much higher in energy than the other empty states, we did not take them into account in our calculations, restricting ourselves to the physically meaningful states. This restriction is further supported by the fact that the LMTO method, like all the other linear methods, does not give accurate results too far away from the Fermi energy, although the inclusion of the so-called combined-correction term (which was not used here) has been shown to extend the validity of the method. Furthermore, because of the broad gap between the sulphur s and p states, we have used two panels in all our calculations in order to treat correctly the low-lying sulphur s states.

3. Electronic band structure

3.1. Non-magnetic calculation

As a first step, we have performed a non-magnetic band-structure calculation. The result is shown in figure 4, both for the 1T and 3R polytypes. One of the striking features is the existence of flat bands sitting in the vicinity of the Fermi energy. Furthermore, the band width decreases when going from the trigonal to the rhombohedral symmetry. These bands are the chromium d bands. In the case of an ideal cubic symmetry, they would be five-fold degenerate. But, since chromium atoms occupy octahedral holes in the 1T and the 3R structures, the corresponding octahedral ligand field splits apart the five d states into the so-called e_g ones with a two-fold degeneracy, and the t_{2g} which are three-fold degenerate. The former are composed of the d_{xz} and d_{yz} states while the latter are formed by the d_{z^2}, d_{xy} and $d_{x^2-y^2}$ orbitals. Note that this decomposition of the e_g and t_{2g} states is different from the usual one (d_{z^2} and $d_{x^2-y^2}$ for e_g and d_{xy}, d_{xz} and d_{yz} for t_{2g}) because, in the present case, the atoms of the octahedron are not on the x, y and z axes. In both calculations shown in figure 4, the Fermi level lies within the t_{2g} bands. Since the d_{xy} and

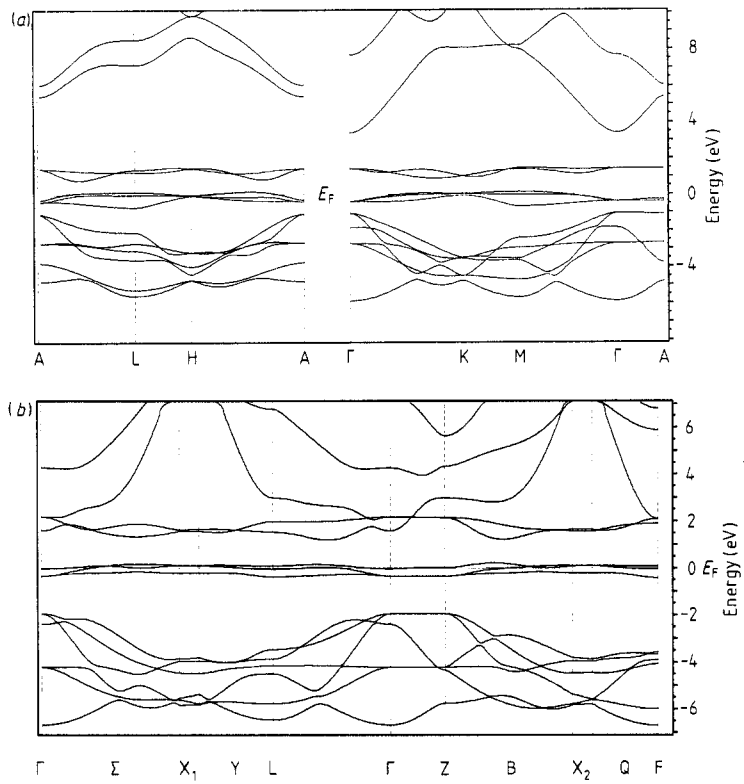

Figure 4. Band structure of non-magnetic (*a*) 1T and (*b*) 3R $NaCrS_2$ polytypes.

$d_{x^2-y^2}$ lie in the Cr planes; they do not significantly overlap with the sulphur p orbitals, whilst the d_{xz} and d_{yz} can hybridise with the sulphur p orbitals. This hybridisation pushes the e_g bands up in energy, above the t_{2g} bands.

Figures 5(*a*) and (*b*) show the corresponding densities of states. One sees at once that in the 3R structure the sulphur p bands occur at higher binding energy than the corresponding S p bands in the 1T structure. In both structures, the Fermi energy is pinned by the t_{2g} bands. Since the local coordination of the 1T and the 3R is the same, the energy shift of the sulphur p bands is due to the differences in the stacking of the layers. Indeed, our calculations show that the Madelung potentials are very different between the two structures. We will further discuss this in § 4.

As a conclusion to this subsection, we can say that the non-magnetic $NaCrS_2$ has been found to be metallic with a high density of states (DOS) at the Fermi energy (>400 states Ryd^{-1}/cell). Because of the high chromium DOS N^{Cr} at the Fermi level and the large exchange interaction of the chromium ions ($I^{Cr} \simeq 1.43$) (Moruzzi *et al* 1978), we find from our calculations that $NaCrS_2$ is unstable ($I^{Cr}N_d^{Cr} \gg 1$) with respect to a magnetic ground state.

3.2. Ferromagnetic solution

We thus performed local spin-density calculations for a ferromagnetic arrangement of the spins. We found a stable solution that has a magnetic moment of $3\mu_B$ for both the 1T

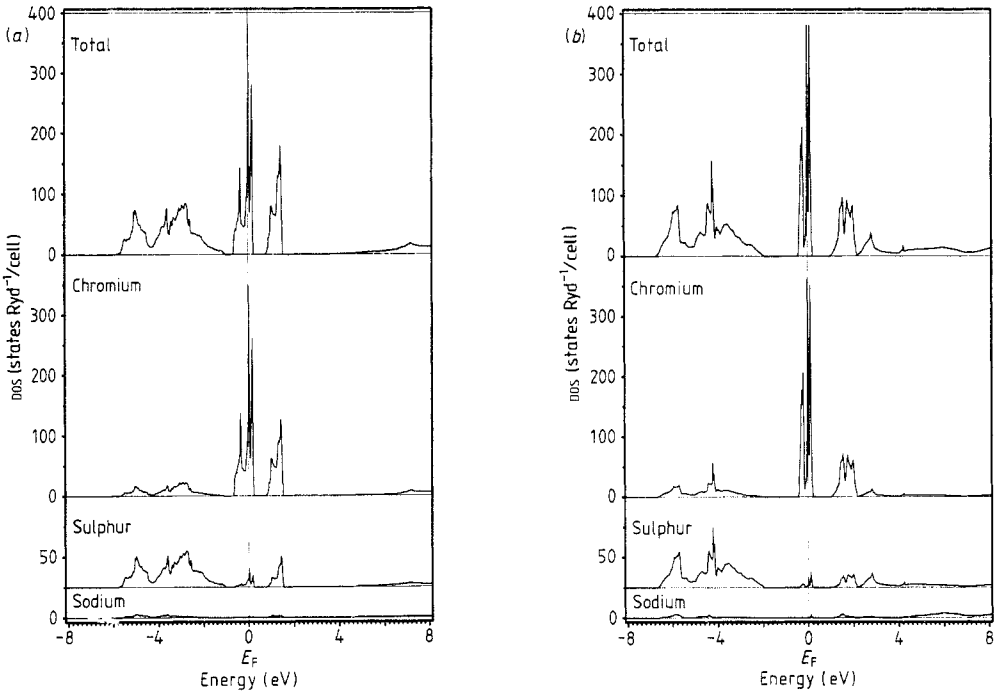

Figure 5. Total and site-decomosed densities of states for non-magnetic (*a*) 1T and (*b*) 3R $NaCrS_2$.

and the 3R structures. This is in agreement with the experiments, where the value of a moment of $3\mu_B$ was found in the magnetic-susceptibility measurements of Blazey and Rohrer (1969) and indirectly from the photoemission experiments of Hughes *et al* (1981).

The electronic structure of ferromagnetic $NaCrS_2$ is insulating (figure 6). We found the Cr t_{2g} bands to be occupied for the majority spin and empty for the minority one (figure 7). This difference in occupation gives rise to the magnetic moment of $3\mu_B$. The gap is between the t_{2g} and the e_g bands of the majority spin, being 0.69 eV in the 1T structure and 1.16 eV in the 3R structure (see table 2). In the 1T structure, the majority t_{2g} bands will overlap with the sulphur p bands whilst they are well separated in the 3R structure. The various band widths and band gaps are listed in table 2 for comparison.

3.3. Antiferromagnetic calculation

It is experimentally known that $NaCrS_2$ is antiferromagnetic, but its exact magnetic structure is still controversial. Indeed, all the authors agree on describing the gross features of the magnetic structure to be ferromagnetic planes that are antiferromagnetically coupled. However, the more detailed spin arrangement has not been settled satisfactorily (Bongers *et al* 1968, Blazey and Rohrer 1969, Engelsman *et al* 1973). As two of the three experimental reports favour the same model, this model has been hailed as the more likely. First proposed by Bongers *et al* (1968), and then refined by Engelsman *et al* (1973), it describes the magnetic coupling as helical, the spins of two adjacent Cr ions within a layer making an angle of 33° with respect to each other. But further experiments including new techniques such as spin-polarised photodiffraction

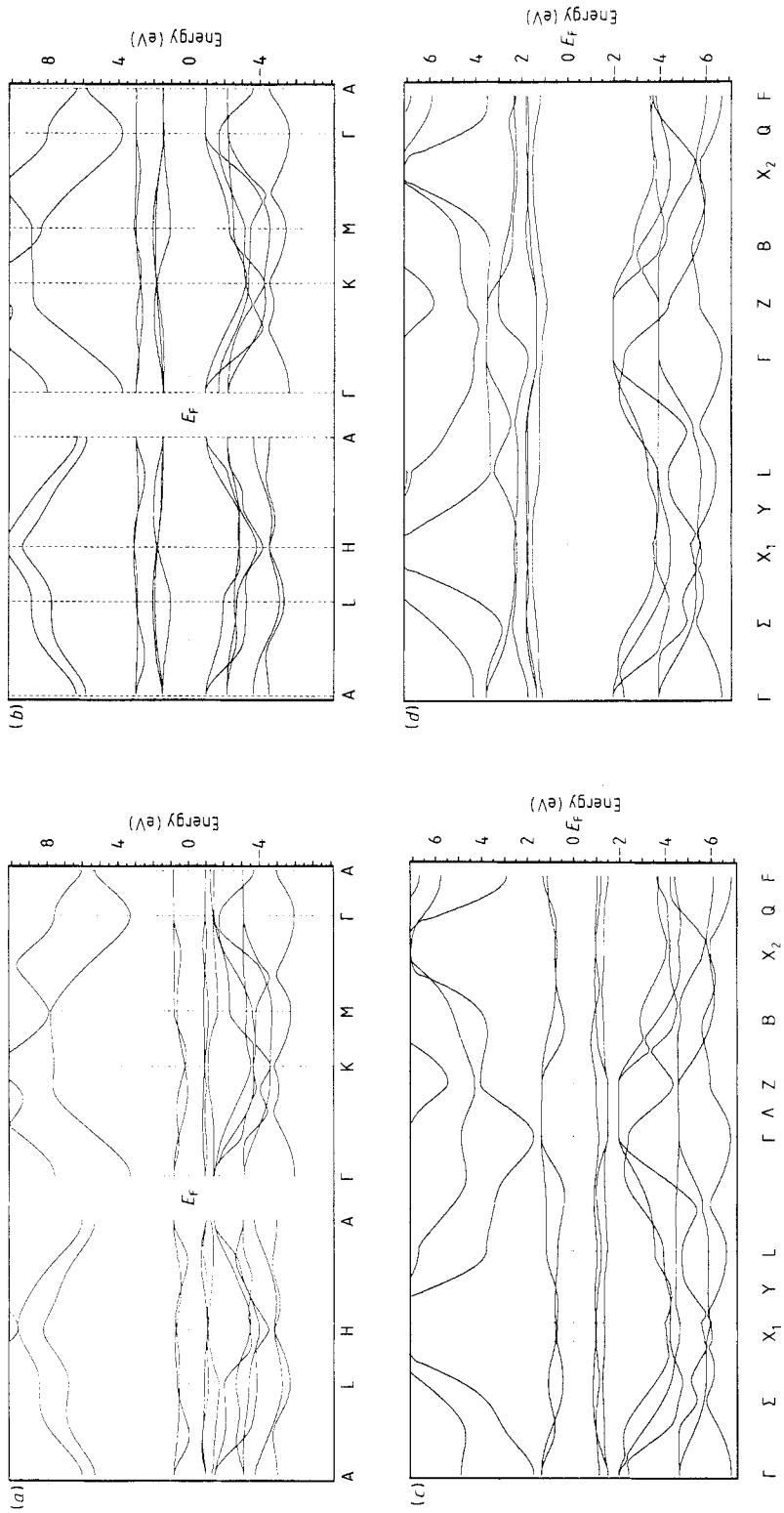

Figure 6. Band structure of ferromagnetic (*a*) 1T and (*b*) 3R $NaCrS_2$.

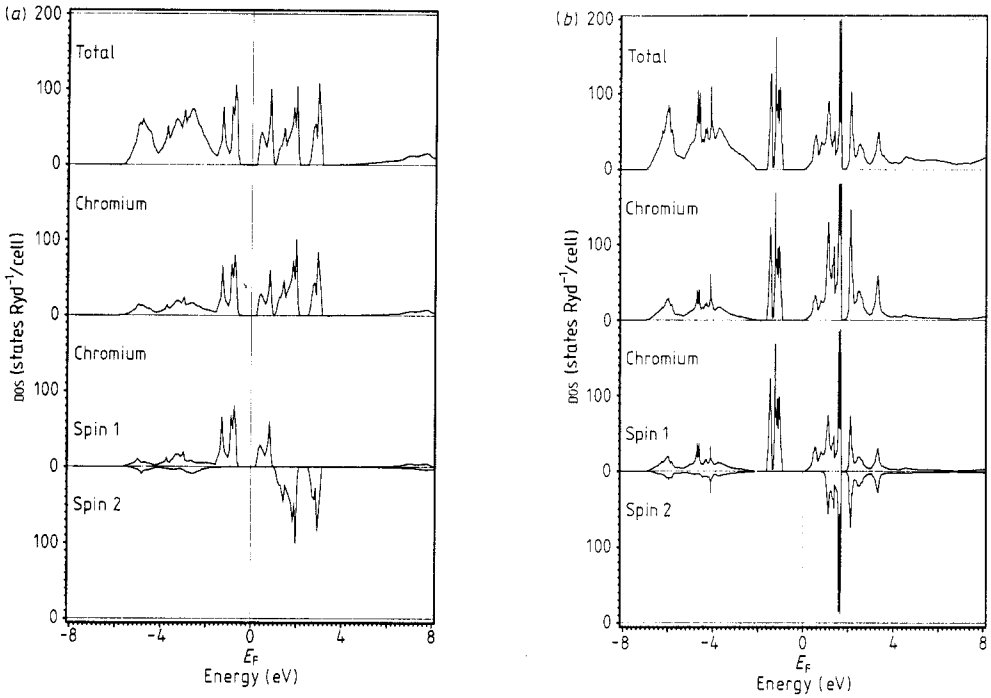

Figure 7. Total, Cr-site and spin-decomposed densities of states of ferromagnetic (*a*) 1T and (*b*) 3R $NaCrS_2$.

Table 2. The band widths and band gaps (in eV) of 1T and 3R $NaCrS_2$ in various states†.

	1T polytype			3R polytype		
	NM	FM	AF	NM	FM	AF
p band width	4.836	(↑) 4.495 (↓) 4.718	4.885	4.736	(↑) 4.886 (↓) 4.729	4.88
p–d gap	0.325	(↑) −0.267 (↓) 1.941	−0.685	1.568	(↑) 0.469 (↓) 2.870	0.479
t_{2g} band width	0.864	(↑) 0.991 (↓) 1.028	(1) 0.853 (2) 1.002	0.536	(↑) 0.721 (↓) 0.941	(1) 0.641
t_{2g}–e_g gap	0.645	(↑) 0.686 (↓) 0.437	(1) 0.962 (2) 0.567	1.050	(↑) 1.163 (↓) −0.118	(1) 1.205
band gap	—	0.686	0.962	—	1.163	1.205
e_g band width	0.702	(↑) 0.853 (↓) 0.620	(1) 0.668 (2) 0.377	—	(↑) 1.001	—
e_g–s gap	1.931	(↑) 2.464 (↓) 0.653	0.590		0.330	

† NM: non-magnetic; FM: ferromagnetic; AF: antiferromagnetic. (↑) denotes majority spin, (↓) denotes minority spin. (1) refers to the lower t_{2g} (or e_g) band and (2) refers to the higher t_{2g} (or e_g) band.

need to be done in order to determine, without any doubt, the exact magnetic structure of $NaCrS_2$.

In our calculations, we considered a ferromagnetic spin arrangement within each layer and the layers coupled to each other antiferromagnetically. This doubled the size

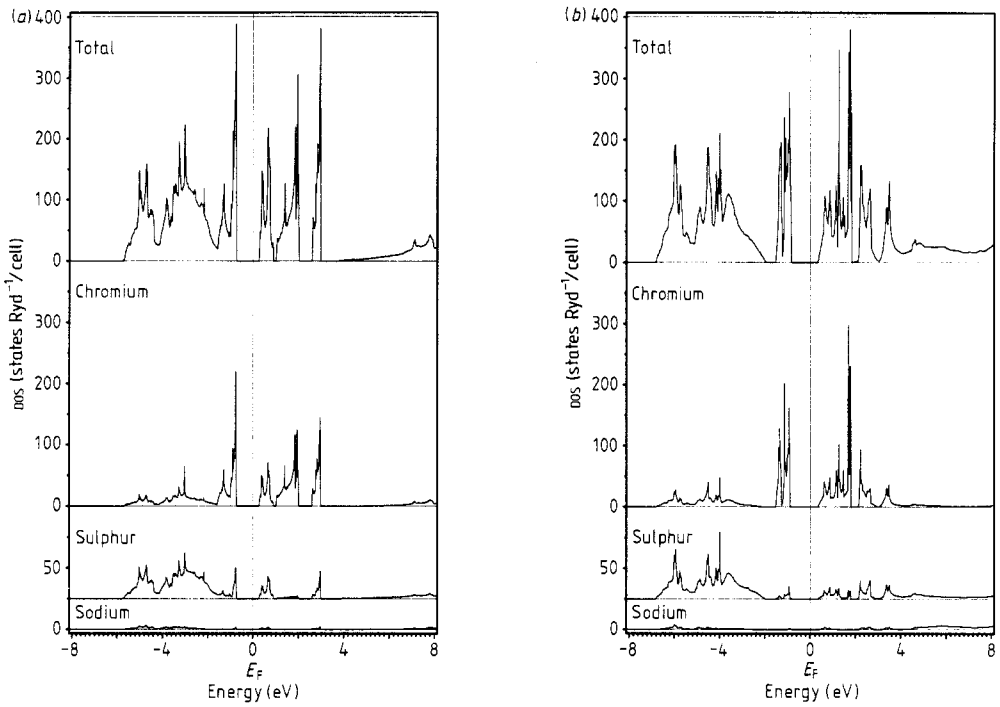

Figure 8. Total and site-decomposed densities of states of antiferromagnetic (*a*) 1T and (*b*) 3R $NaCrS_2$.

of the unit cell along the *c* direction (because of our neglect of the spin–orbit coupling, the spin direction relative to the crystal axes could not be determined).

The densities of states of 1T and 3R antiferromagnetic $NaCrS_2$ are shown in figure 8. The antiferromagnetic coupling should be small and, therefore, ferromagnetism should not be very different for two consecutive Cr^{3+} layers. Indeed, if we superpose the majority and minority spin DOS for the ferromagnetic state, we find that this composite DOS is very similar to that of the antiferromagnetic state. Again, the semiconducting gap is bigger and the sulphur-dominant bands are shifted further downwards in the real 3R structure than in the hypothetical 1T polytype. However, the gap remains twice as small as the experimental direct band gap, but this order of magnitude is a feature common to all the local density- (and more generally, density-functional-theory-) based band-structure methods (e.g. Godby *et al* 1987).

Inspection of the bands (figure 9) shows that the d orbitals are slightly more localised in the case of the antiferromagnetic coupling. This is further visible in table 2 where the band gap and the width of the e_g and t_{2g} bands are given for the two polytypes studied and for both magnetic structures.

3.4. Ferromagnetism against antiferromagnetism

Table 3 gives the total energy and its decomposition for all the cases studied. The total energy E_T has been decomposed in the following way: $E_T = E_B + E_C + E_{XC}$ where E_B, E_C and E_{XC} are respectively the band, Coulomb and exchange-correlation terms. As can

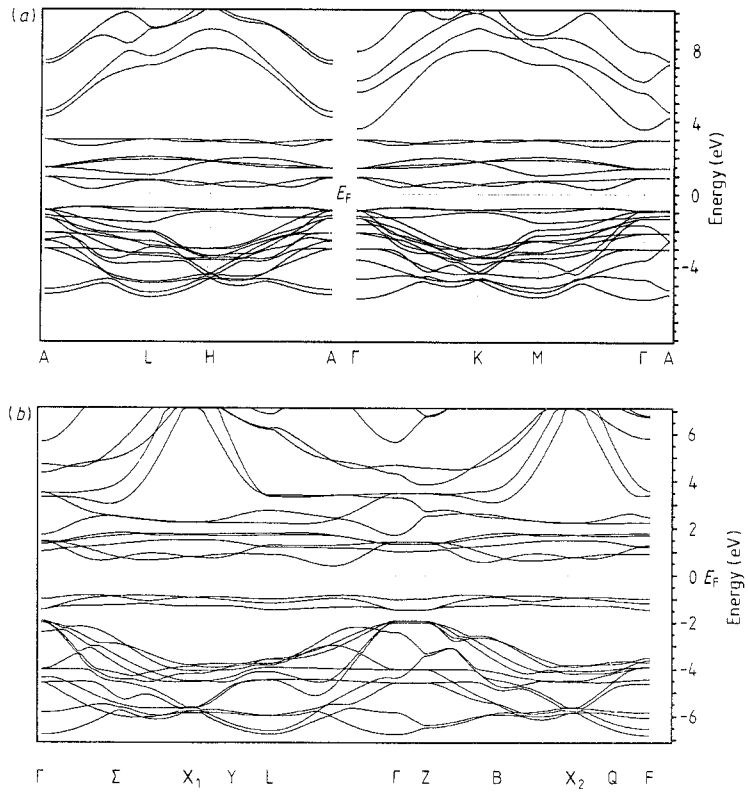

Figure 9. Band structure of antiferromagnetic (*a*) 1T and (*b*) 3R $NaCrS_2$.

Table 3. Total energy E_T, and its contributions E_B (band), E_C (Coulomb), E_{XC} (exchange and correlation) for the 1T and 3R structures and for the different magnetic structures. E_{MAD} denotes the Madelung contribution to E_C.

Calculation	*K*-points	E_T	E_B	E_C	(E_{MAD})	E_{XC}
Non-magnetic 1T	112	−63.7481	−11.0271	−31.7079	(0.6777)	−21.0132
Ferromagnetic 1T	112	−63.8424	−11.1313	−31.4501	(0.7294)	−21.2609
Antiferromagnetic 1T	84	−63.8523	−11.1617	−31.4362	(0.7245)	−21.2544
Non-magnetic 3R	75	−63.9159	−10.4077	−32.5825	(0.1683)	−20.9257
Ferromagnetic 3R	75	−64.0203	−10.5856	−32.2873	(0.2144)	−21.1473
Antiferromagnetic 3R	45	−64.0249	−10.5917	−32.2828	(0.2334)	−21.1503
	105	−64.0264	−10.5938	−32.2825	(0.2339)	−21.1500

be seen from this table, the non-magnetic structure is less stable than the magnetic ones: E_B and E_{XC} are much lower in the magnetic structures at the expense of E_C, giving a net energy gain. Moreover, we can see from this table that the antiferromagnetic structure is more stable than the ferromagnetic one. For the antiferromagnetic 3R structure, the results of two calculations with a different number of *K*-points being given in order to demonstrate that the increased stability is not an artefact coming from the changes in the number of *K*-points. The antiferromagnetic solution is preferred because of a further

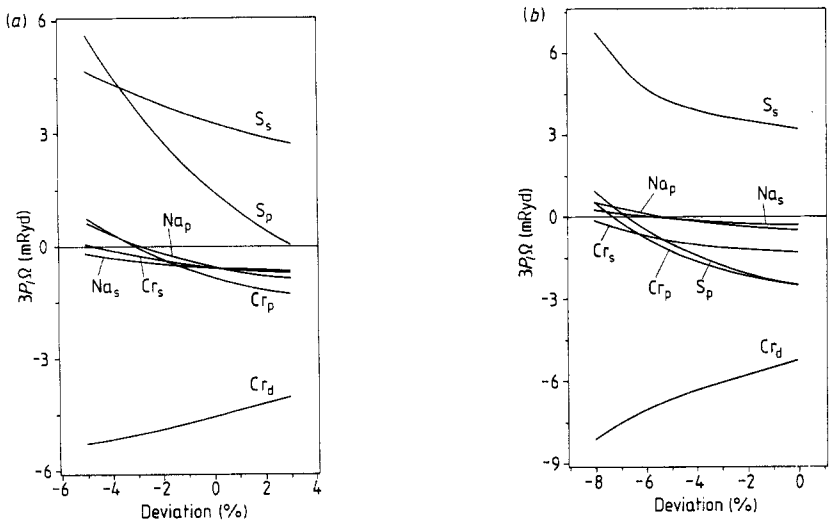

Figure 10. The angular-momentum and site-decomposed electronic pressures (P_l) as a function of lattice constant in non-magnetic (*a*) 1T and (*b*) 3R $NaCrS_2$. Ω is the unit cell volume.

gain in energy in the E_B term. This is correlated with the slight increase of the band gap that is due to a hybridisation between majority and minority spins of antiferromagnetically coupled layers. We also find the 3R polytype to be much more stable than the 1T structure, whatever the magnetic arrangement assumed.

4. Chemical bonding

In figure 10 the partial pressures for the 1T and the 3R polytypes are plotted. In both cases, the bonding is dominated by the attraction of the chromium d electrons and the repulsion of the sulphur s electrons, and, for the 1T structure, by the repulsion of the S p electrons as well. All the other states have partial pressures close to zero and, therefore, they are less important in the bonding.

We have also calculated the variations of the total energy with the lattice parameter, in order to find the theoretical lattice constant. For both structures, this lattice constant agrees with the experimental value to within one or two per cent. However, a change of the sphere size will induce a change of the theoretical lattice constant, as shown in figure 11. Here, we have calculated the variations of the total energy with the lattice constant in the case of the 1T polytype for six different sets of sphere sizes. The radius of the sodium sphere was kept at a constant value of 3.0028 au in all calculations but one. The exception is the dotted curve, where the four spheres (Na, Cr and 2 S) have been given the same radius, which is different from the 3.0028 one because the total volume of the spheres must equal the volume of the unit cell (this is the atomic sphere approximation). It is obvious from this figure that the bigger the chromium size, the smaller the lattice constant. Similar calculations with two different chromium-sphere sizes suggest that this trend remains valid for the 3R structure.

The fact that the theoretical lattice constant can be varied substantially (figure 11) by changing the atomic-sphere sizes is not very satisfactory: it is a consequence of the change in the overlap of the ASA spheres. However, the fact that a better agreement

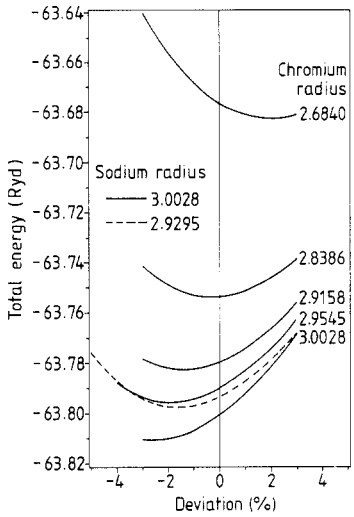

Figure 11. Total energy as a function of lattice constant in non-magnetic 1T structure for different Cr-atomic radii.

Table 4. The electronic charges in the Cr, S and Na spheres for the 1T and 3R structures and the different magnetic structures. Note that the sphere radii in the 1T and 3R structures are the same: Cr = S = Na = 3.0534 au.

Calculation	Cr	S	Na
Non-magnetic 1T	23.8048	16.1817	10.8319
Ferromagnetic 1T	23.7563	16.2053	10.8301
Antiferromagnetic 1T	23.7605	16.2014	10.8369
	23.7614	16.2007	10.8374
Non-magnetic 3R	24.1244	16.1139	10.6476
Ferromagnetic 3R	24.0753	16.1339	10.6527
Antiferromagnetic 3R	24.0771	16.1344	10.6526
	24.0809	16.1341	10.6526

with experimental results is obtained with a smaller chromium radius indicates that chromium wants to be a small atom and, therefore, that its orbitals are more localised. Although the theoretical lattice constant is sensitive to the choice of the chromium-sphere size, we found that the band structure remained essentially unaltered. The set of radii used for the calculations reported in § 3 is the one for which each sphere has the same radius as the other ones (Cr = S = Na = 3.0534 au).

For comparison, the electronic charges on the atoms for the various calculations are given in table 4. The first trend shown by this table is that, for both polytypes, the number of electrons on the chromium atom reduces and the corresponding charge is transferred to the sulphur atom when going from the non-magnetic to the magnetic structure. This charge transfer decreases the bonding and is seen together with an expansion of the lattice. Furthermore, the reduction of the number of electrons on the chromium atom means that the Cr d electrons will be more localised; this is effectively what is seen in table 2 where the band width decreases from the non-magnetic structure to the magnetic ones. Another trend revealed by table 4 is the transfer of electrons from the sodium to the chromium atom when the 1T polytype is changed into the 3R one. This charge

transfer is then of about $0.3\,e$ and is a consequence of the large differences in the Madelung potential between the 3R and 1T structures. Indeed, table 3 shows a large difference in the Madelung energy of the order of 0.5 Ryd between the two types of crystalline structure. This difference is sufficient for the E_C term of the total energy to overcome the loss in band energy (E_B) and make the 3R structure energetically more favourable.

5. Comparison with photoemission

Angle-resolved photoemission experiments have been performed on $NaCrS_2$ by Hughes *et al* (1981). They were able to map the energy bands in the ΓM direction of the basal plane. They see the chromium d bands below the top of the sulphur p bands, in contradiction to the findings of Blazey and Rohrer (1969) (from optical transitions), who positioned the chromium d bands 0.5 eV *above* the top of the sulphur p bands. This discrepancy is presumably due to the shift to higher binding energies of narrow bands in the photoemission process (Jordan and Durham 1989). However, the photoemission data for the band-like states can be directly compared with our band-structure results (Hughes and Liang 1973). These photoemission data available for $NaCrS_2$ suggest that the top of the sulphur p bands occur at approximately 1 eV binding energy with a width of 5.5 eV.

We find our band structure calculations to be in excellent agreement with the sulphur-related features of the photoemission data: the top of the sulphur p bands is at about 1 eV below the top of the valence band, and these bands have a width of 4.9 eV. The narrow chromium t_{2g} bands are 0.5 eV above the top of the sulphur p bands, in accord with the findings for the optical measurements (Blazey and Rohrer 1969). Our calculations indicate that the binding energy of the t_{2g} bands is dependent on the inter-layer arrangements. In the 1T structure, these t_{2g} bands overlap with the sulphur p bands.

6. Summary

The local spin-density band model gives an excellent description of the ground-state properties of antiferromagnetic and semiconducting $NaCrS_2$, such as the electronic charge distribution and the magnetic moment. The band structure consists of narrow chromium d bands separated from a broad sulpher p band. The calculated local spin moment is $3\mu_B$/Cr, in agreement with experiment. The value of the moment is determined by the intra-layer magnetic interactions, whilst the inter-layer interactions are responsible for the antiferromagnetic ordering. The competition of the attraction of the chromium 3d electrons and the repulsion of the sulphur s electrons is responsible for the chemical bonding. The band model also correctly predicts the 3R structure as the ground state against a hypothetical 1T structure. The larger Madelung energy makes the 3R structure energetically more favourable than the 1T structure.

We have demonstrated that the LMTO–ASA band model is capable of giving a unified and quantitative description of the band-like and localised features of the electronic structure of $NaCrS_2$. The dependence of the theoretical lattice constant of $NaCrS_2$ on the Cr Wigner–Seitz sphere radius is a shortcoming of the LMTO–ASA method and could be overcome by a better method, such as the KKR method. The KKR method might also provide the required increase in accuracy for the investigation of the highly complex

spin structures of $NaCrS_2$, of which we have only studied the two simplest structures in this paper.

Acknowledgement

Some of this work was carried out while one of us (DS) held a fellowship under the Royal Society European Science Exchange Programme.

References

Andersen O K 1975 *Phys. Rev.* B **12** 3060
—— 1984 *The Electronic Structure of Complex Systems* ed. P Phariseau and W M Temmerman (New York: Plenum)
Andersen O K, Jepsen O and Glotzel D 1985 *Highlights of Condensed Matter Theory* ed. F Bassani, F Fumi and M P Tosi (Amsterdam: North-Holland)
Benesh G A, Wooley A M and Umrigar C J 1985 *J. Phys. C: Solid State Phys.* **18** 1595
Blazey R W and Rohrer H 1969 *Phys. Rev.* **185** 712
Bongers P F, van Bruggen C F, Koopstra J, Omloo W P F A M, Weigers G A and Jellinek F 1968 *J. Phys. Chem. Solids* **29** 977
Engelsman F M R, Wiegers G A, Jellinek F and van Laar B 1973 *J. Solid State Chem.* **6** 574
Friend R H and Yoffe A D 1987 *Adv. Phys.* **36** 1
Godby R W, Schlüter M and Sham L 1987 *Phys. Rev.* B **36** 6497
Guo G Y and Liang W Y 1987 *J. Phys. C: Solid State Phys.* **20** 4315
Hohenberg P and Kohn W 1964 *Phys. Rev.* **136** 864
Hughes H P and Liang W Y 1973 *J. Phys. C: Solid State Phys.* **6** 1684
Hughes H P, Parke A W, Williams R H and Barry J J 1981 *J. Phys. C: Solid State Phys.* **14** L1103
Jordan R G and Durham P J 1989 *Alloy Phase Stability* ed. G M Stocks and A Gronis (Dordrecht: Kluwer Academic)
Kohn W and Sham L J 1965 *Phys. Rev.* A **140** 1133
Khumalo F S and Hughes H P 1980 *Phys. Rev.* B **22** 4066
Liang W Y 1986 *Intercalation in Layered Materials* ed. M S Dresselhaus (New York: Plenum)
Moruzzi V L, Janak J F and Williams A R 1978 *Calculated Electronic Properties of Metals* (Oxford: Pergamon)
Rüdorff W and Stegemann K 1943 *Z. Anorg. (Allg.) Chem.* **251** 376
Skriver H L 1984 *The LMTO Method* (Berlin: Springer)
Thiry P, Chandesris D, Lecante J, Guillot C, Pinchaux R and Petroff Y 1977 *Phys. Rev. Lett.* **19** 1632
van Bruggen C F, Haange R J, Wiegers G A and de Boer D K G 1980 *Physica* B **99** 166
von Barth U and Hedin L 1972 *J. Phys. C: Solid State Phys.* **5** L733
Wilson J A and Yoffe A D 1969 *Adv. Phys.* **18** 193